Characterization of a coupled DNA replication and translesion synthesis polymerase supraholoenzyme from archaea

Matthew T. Cranford[1],[†], Aurea M. Chu[1],[†], Joshua K. Baguley[1], Robert J. Bauer[2] and Michael A. Trakselis[1],[*]

[1]Department of Chemistry and Biochemistry, Baylor University, Waco, TX 76798, USA and [2]Department of Chemistry, University of Pittsburgh, Pittsburgh, PA 15260, USA

ABSTRACT

The ability of the replisome to seamlessly coordinate both high fidelity and translesion DNA synthesis requires a means to regulate recruitment and binding of enzymes from solution. Co-occupancy of multiple DNA polymerases within the replisome has been observed primarily in bacteria and is regulated by post-translational modifications in eukaryotes, and both cases are coordinated by the processivity clamp. Because of the heterotrimeric nature of the PCNA clamp in some archaea, there is potential to occupy and regulate specific polymerases at defined subunits. In addition to specific PCNA and polymerase interactions (PIP site), we have now identified and characterized a novel protein contact between the Y-family DNA polymerase and the B-family replication polymerase (YB site) bound to PCNA and DNA from *Sulfolobus solfataricus*. These YB contacts are essential in forming and stabilizing a supraholoenzyme (SHE) complex on DNA, effectively increasing processivity of DNA synthesis. The SHE complex can not only coordinate polymerase exchange within the complex but also provides a mechanism for recruitment of polymerases from solution based on multi-equilibrium processes. Our results provide evidence for an archaeal PCNA 'tool-belt' recruitment model of multienzyme function that can facilitate both high fidelity and translesion synthesis within the replisome during DNA replication.

INTRODUCTION

To ensure accurate and faithful DNA synthesis, the DNA replisome must maintain a certain plasticity, such that enzymes can be exchanged to overcome any obstacles to replication. Although the bulk of DNA synthesis is performed by high fidelity B-family (archaea and eukaryotes) or C-family (bacteria) DNA polymerases that ensure genomic integrity, DNA damage encountered in the template strand is replicated using lower fidelity Y-family translesion (TLS) DNA polymerases (1,2). In eukaryotes, multiple TLS polymerases have evolved to provide specificity and accuracy of DNA synthesis across a broad range of lesions in spite of the type of damage (3,4). However, bacteria and archaea generally contain one or two translesion DNA polymerases with broader lesion specificity.

In both archaea and eukaryotes, the processivity clamp, PCNA, interacts with many protein partners that contain a PCNA interacting peptide (PIP) motif that binds to a hydrophobic pocket on the front face of PCNA (5). This common interaction site on PCNA is utilized to localize proteins not only for DNA replication but also for translesion synthesis, mismatch repair, nucleotide excision repair, chromatin remodeling, and cell cycle control, making PCNA an important localization point for many DNA related processes (6,7). In eukaryotes, although specific mechanisms may differ between yeast and mammals, optimal TLS activity includes the monoubiquitinylation (mUb) of PCNA (8,9). The hypothesis is that the combination of mUb and PIP binding provides greater binding specificity and selectivity for TLS polymerases. Eukaryotic Y-family TLS polymerases, pol η, pol κ, pol ι, all contain both PIP sites and ubiquitin binding domains (UBD) (3,10). mUb-PCNA has been shown to not only increase the localization of these TLS polymerases to sites of damage (11,12), but it also aids in the resistance to UV sensitization of cells (13). These *in vivo* results are validated by the increased kinetic polymerization ability of TLS polymerases with mUb-PCNA compared to unmodified PCNA (14,15). Therefore, the combination of PIP and UBD sites increases the localization and

[*]To whom correspondence should be addressed. Tel: +1 254 710 2581; Fax: +1 254 710 4272; Email: michael_trakselis@baylor.edu
[†]These authors contributed equally to this work as first authors.
Present address: Robert, J. Bauer, DNA Enzymes Division, New England Biolabs, Inc., Ipswich, MA 01938-2723, USA.

stability of TLS polymerases at sites of DNA damage in eukaryotes.

Although bacteria and archaea also possess multiple DNA polymerases including Y-family TLS polymerases, the processivity clamps in these organisms do not seem to be modified with ubiquitin or any other posttranslational modifications. Instead, the PIP binding site (in archaea) (16,17) or the equivalent hydrophobic patch on the β-clamp (in bacteria) (18) are the primary interaction sites for both high and low fidelity DNA polymerases within both domains. In addition to clamp binding, direct contacts between polymerases (Pol III and Pol II or Pol IV) have been identified that are important for polymerase switching and translesion synthesis in bacteria (19,20). Although an initial interaction between PolB1 and PolY has been identified in archaea (21), its mechanistic role in polymerase exchange or TLS has not been described making comparisons with either the bacterial or eukaryotic domain impossible. However, homoligomeric contacts within single archaeal DNA polymerases have been described (22,23), providing a potential for heteroligomeric polymerase contacts. Barring these secondary interaction sites, there would be direct competition and thermodynamic equilibria/competition for individual polymerase molecules binding to PCNA and DNA, potentially impacting processivity and fidelity of DNA synthesis (22,24).

Because the eukaryotic DNA processing components seemed to have emerged from a common ancestor in archaea (25,26), the archaeal DNA replication enzymes are a *de facto* relevant model system for understanding mechanism of action within the replisome. In fact, *Sulfolobus solfataricus* (*Sso*) Dpo4 (PolY) has been one of the most intricately studied DNA polymerases with regards to its structure/function, kinetics, and template lesion bypass specificities (27–37). The heterotrimeric *Sso*PCNA123 clamp can provide for more specific interactions of proteins with individual subunits in a 'tool-belt' configuration (38–40), similar to that described for the bacterial system (41). *Sso*PolB1 is considered to be the main DNA replication polymerase and interacts specifically with *Sso*PCNA2 (38,42), while *Sso*Dpo4 (PolY) is the primary TLS polymerase and interacts specifically with *Sso*PCNA1 (43). In addition, direct contacts between PolB1 and PolY have also been observed but not functionally characterized (21). Therefore, the potential for a coordinated PolB1/PolY/PCNA123 supraholoenzyme (SHE) in *Sso* is possible and would provide valuable insight into the polymerase exchange mechanism in archaea.

In this report, we have not only detected the presence of a *Sso* SHE complex using analytical gel filtration and presteady-state stopped flow FRET, but we have also validated the activity and polymerase exchange using both kinetic replication and processivity assays. Interaction between PolB1 and PolY within the SHE occurs at both PIP sites on PCNA2 and PCNA1, respectively, as well as a novel YB binding site directly between PolY-PolB1 polymerases. Addition of PolY stabilizes the SHE complex on DNA and increases processivity of DNA synthesis. Although direct polymerase solution equilibrium competition occurs for binding to DNA, the presence of both the PIP and YB interaction sites in the SHE increases the ability to directly exchange and regulate polymerase contacts with the primer-template. Altogether, this work identifies the presence of a novel YB interaction site that is important in coordinating polymerase switching for low and high fidelity synthesis within a novel supraholoenzyme complex, providing significant implications for polymerase recruitment and lesion bypass during replication.

MATERIALS AND METHODS

Materials

Oligonucleotides used (Supplemental Table S1) were purchased from IDT (Coralville, IA, USA). Fluorescently labeled DNA was HPLC purified by IDT. ATP was from Sigma-Aldrich (St. Louis, MO, USA). ^{32}P-γ-ATP was from PerkinElmer (Waltham, MA, USA). Alexa Fluor 488® (A^{488}) and Alexa Fluor 594® (A^{594}) C5 maleimides were from ThermoFisher (Pittsburgh, PA, USA). All other chemicals, buffers, and media were analytical grade or better.

Cloning and protein purification

Sso PolB1, RFC and PCNA123 and their mutants were purified as described previously (44). *Sso*PolY mutants were created using a standard Quikchange protocol from pET11-Dpo4 (22,28) using KAPA DNA polymerase (Kapa Biosystems, Wilmington, MA, USA). Primers are listed in Supplemental Table S1. Mutations were confirmed by DNA sequencing (ICMB, UT Austin). PolY WT and mutants were purified essentially as described previously (22) using autoinduction (45) in Rosetta 2 cells (Novagen EMD Millipore, Billerica, MA, USA) followed by HiTrap MonoQ, Heparin, and Superdex S-200 columns on a AKTA Pure FPLC chromatography system (GE Healthcare Life Sciences, Marlborough, MA, USA). All PolY mutants retain near wild-type activity on their own and within a PolY HE complex (data not shown).

Analytical gel filtration

Analytical gel filtration experiments were conducted using a Superdex 200 10/300 GL column (GE Healthcare Life Sciences) equilibrated in Buffer A (20 mM HEPES–NaOH (pH 7.0), 50 mM NaCl, 10% β-mercaptoethanol). Calibration of the Superdex 200 10/300 GL column was performed by running molecular ruler standards consisting of Thyroglobulin (165 kDa, Sigma), Conalbumin (75 kDa, GE Healthcare Life Sciences), Albumin (43 kDa, Sigma), Myoglobin (17.6 kDa, Sigma) and Vitamin B12 (1.4 kDa, Sigma). The standard calibration curve was created by plotting retention volume data against the logarithm of the molecular weights of the calibration proteins and was fitted by linear least squares. Five hundred microliters samples consisting of 5 μM of each indicated component (PolB1, PolY, PCNA123, RFC, DNA21/31) and 1.6 mM ATP were mixed, nutated at room temperature for 10 min, and injected in the Superdex column (4°C). Protein elution was monitored at 280 nm and fractions collected at regular intervals.

Western blot analysis

Analytical gel filtration fractions of SHE and PolY HE were separated in 10% SDS-PAGE, transferred onto PVDF membranes, and probed with antibodies against PolB1 or PolY (1:4000). Proteins of interest were detected with HRP-conjugated anti-rabbit (1:5000) and visualized with the Pierce ECL western blotting substrate (Thermo Scientific, Rockford, IL, USA), using ImageQuant LAS 4000 (GE Healthcare Life Sciences) according to the manufacturer's instructions.

Protein fluorescent labeling

Proteins were fluorescently labeled at a single accessible cysteine residue with either A^{488} or A^{594} maleimides as described previously (44). PolB1 has three native cysteines: C538 and C556 in a disulfide bond and a single solvent accessible C67. C67 was mutated to Ser in favor of moving the labeling position towards the C-terminus (C67S/S740C). Single cysteines were introduced into *Sso*PCNA subunits [PCNA1 (S191C), PCNA2 (S92C)] and labelled similarly. *Sso*Dpo4 (PolY) was labelled at a single native C31 (46). Proteins were dialyzed into their storage buffer free of β-mercaptoethanol before adding 1.2- to 5-fold molar excess dye. Reactions were allowed to proceed for 2 h at room temperature or overnight at 4°C. Labeled proteins were separated from free dye using a 1 ml G-25 column (GE Healthcare Life Sciences), and/or extensive dialysis in labeling buffer. Labeling efficiencies were calculated from a ratio of concentrations (dye:protein) using the extinction coefficients and generally exceeded 95%.

Steady-state FRET

Steady-state fluorescence spectroscopy was performed on a FluoroMax-4 spectrofluorimeter (HORIBA Jobin Yvon). WT or Y122P PolY labeled with A^{488} at 20 nM was titrated at room temperature with increasing concentrations of PolB1 labeled with A^{594} as indicated in the figure legends. The fluorescence emission spectra (505–650 nm) were collected with an excitation wavelength of 485 and 4 nm slits after each PolB1 addition. PolB1^{594} titrations in the presence of unlabeled PolY were also performed similarly and subtracted from the donor/acceptor spectra. The quenching at 517 nm normalized to the donor-only intensity (v) was plotted as a function of PolB1 concentration and fit to the following equation:

$$v = 1 - \frac{\Delta F \times [Pol\,B1]}{K_d + [Pol\,B1]} \qquad (1)$$

where ΔF is the change in fluorescence amplitude, $[PolB1]$ is the protein concentration, and K_d is the dissociation constant calculated using KaleidaGraph (v4.5, Synergy Software). Multiple titrations were performed and averaged included with standard error before fitting.

Presteady-state FRET

Stopped-flow fluorescence experiments were performed on an Applied Photophysics (Leatherhead, UK) SX.20MV in fluorescence mode at a constant temperature of 22°C. Template DNA (31mer) was labeled at the 3′ end with A^{488} by IDT. A 21 base primer was annealed and complementary to the 3′ end of the template. Final concentrations of components after mixing were PolB1 (0.4 μM), RFC (0.4 μM), DNA (0.2 μM), ATP (0.3 mM), and PolY (0.4 μM), unless indicated otherwise. The samples were excited at 490 nm, and a 590-nm-cutoff filter was used to collect 4000 oversampled data points detecting only A^{594} emission over single or split-time bases. The slits were set at 3 mm for both excitation and emission. At least seven traces were averaged for each experiment and performed multiple times and on multiple occasions. The observed averaged traces were fit to one, two or three exponentials using the supplied software. Below is the equation for a double exponential fit:

$$v = a_1 \cdot e^{-k_1 t} + a_2 \cdot e^{-k_2 t} + C \qquad (2)$$

where a is the amplitude change, k is the exponential rate, t is time, and C is a constant for the amplitude.

In vitro replication and processivity assays

Polymerase replication and processivity assays were performed as previously described (44), with the following modifications. PolB1 (0.2 μM), PCNA (2 μM), RFC (0.4 μM) and ATP (0.2 mM) were loaded onto primed M13mp18 DNA (18 nM) to form the PolB1 HE. A M13 primer was 5′ end labeled with ^{32}P-γ-ATP (PerkinElmer, Waltham, MA) using Optikinase (Affymetrix, Santa Clara, CA) according to manufacturer's instructions. PolY was added (at indicated concentrations) and incubated for 5 min, before initiating the reaction with 0.2 mM dNTPs. Single-turnover processivity assays were simultaneously initiated with 0.2 mM dNTPs and a 5000-fold excess salmon sperm DNA trap (3 mg/ml). DNA products were separated on either a 0.8% or 2.5% alkaline agarose gel depending on expected product length and dried under vacuum at 80°C for 1 h. Gels were exposed to a phosphorscreen (GE Healthcare Life Sciences) for a minimum of 4 h, imaged using a Storm 820 Phosphorimager (GE Healthcare Life Sciences), and the data analyzed using ImageQuant software (v.5.0, GE Healthcare Life Sciences). Quantification of the lane profiles from multiple experiments were calibrated to the 1kb DNA ladder (Promega, Madison, WI) to determine DNA product lengths.

RESULTS

Detection of the supraholoenzyme (SHE) complex

As a means to follow composition and stability of the DNA polymerase holoenzyme complexes, we utilized analytical gel filtration chromatography (Figure 1A). The heteropentameric *Sso* clamp-loader (RFC), consisting of four subunits of RFCS (small) and 1 subunit of RFCL (large), alone elutes around 12 ml with a total molecular weight of 197 760 g/mol. RFC-directed loading of PCNA (individual subunits 1, 2 and 3) onto DNA is apparent at 10.5 ml. The broad spread of signal from 10 to 14 ml most likely indicates dynamic loading/dissociation of PCNA on DNA and interactions with RFC as well as RFC and
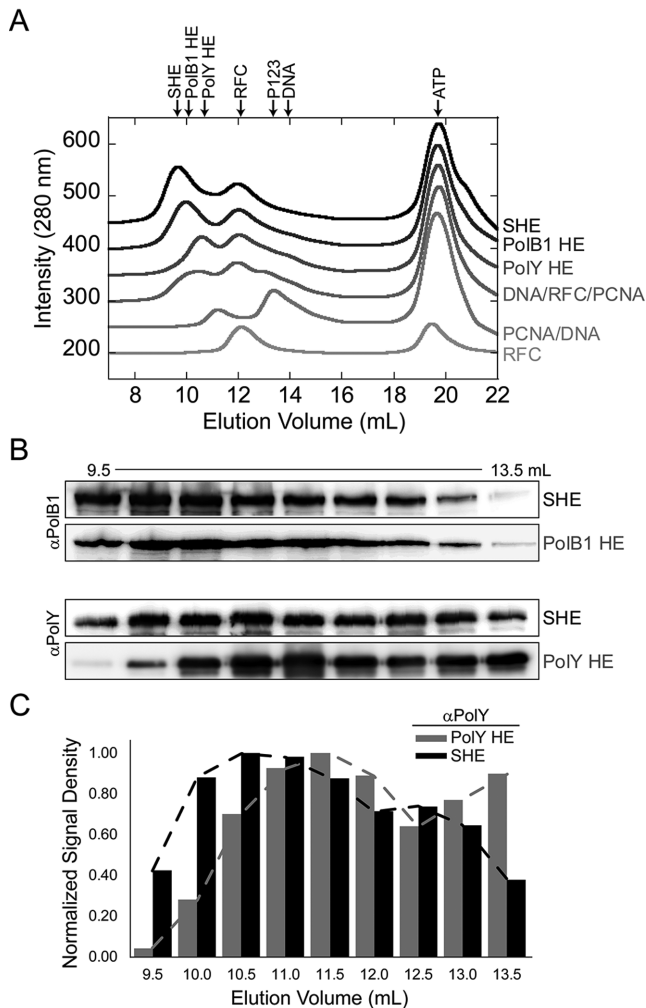
Figure 1. Detection of Supraholoenzyme (SHE) Complex by Analytical Gel Filtration. (**A**) Size exclusion chromatography profile of the different protein/DNA complexes performed as described in Materials and Methods. PolY holoenzyme (PolY HE) consists of PolY/ DNA/RFC/PCNA123. PolB1 HE consists of PolB1/DNA/RFC/PCNA123. SHE consists of PolB1HE/PolY. ATP was included in all reactions for RFC-directed HE formation as well as an internal standard to account for drift in the elution profile. (**B**) Western-blot analysis of αPolB1 and αPolY in SHE and PolB1 or PolY HE fractions. (**C**) Relative quantification of PolY compared between SHE and PolY HE.

PCNA123 alone. Formation of the PolY HE complex includes PolY/PCNA123/DNA at 10.6 ml with RFC dissociated from this complex. Similarly, the PolB1 HE consisting of PolB1/PCNA123/DNA forms at 10.5 ml (Figure 1B) with RFC dissociated as also indicated previously (44). Interestingly, addition of PolY to the PolB1 HE shifts the main peak to 9.7 ml indicative of a higher order SHE complex consisting of both PolY and PolB1 bound to PCNA and DNA. A western blot of the gel filtration fractions shows the shift and presence of PolY in the earlier eluting fractions within the SHE complex (Figure 1B and C).

In order to directly monitor interactions between PolB1 and PolY by fluorescence resonance energy transfer (FRET), we labelled single cysteine positions on both proteins with fluorescent dyes. All proteins were active after labeling and were able to stimulate the activity of the respective PolB1 and PolY holoenzymes (data not shown). Titration of PolY labelled at C31 with Alexa 488 (A^{488}) with PolB1 labeled at C740 with Alexa 594 (A^{594}) showed fluorescence quenching and acceptor sensitization of the donor fluorescence consistent with an interaction between these two polymerases (Figure 2A). Steady-state FRET experiments were also performed in reverse (PolY^{594} titrated into PolB^{488}) with similar results and K_d (data not shown). Quantification of the normalized donor quenching at 517 nm as a function of [PolB1^{594}] was fit to Equation (1) to give a $K_d = 0.14 \pm 0.02$ μM (Figure 2B).

The interaction between PolB1 and PolY was also monitored by presteady-state FRET using a stopped-flow instrument. Rapid mixing of equal molar PolB1^{488} and PolY^{594} (0.4 μM final) shows a biphasic fluorescence increase consistent with a direct interaction between polymerases (Figure 2C). Doubling or quadrupling the concentration of PolY^{594} does not significantly affect the observed rate constants, k_1 and k_2, consistent with second order conformational change processes. Importantly, these experiments formed the basis for directly monitoring PolB1–PolY interactions within a SHE complex by FRET.

Recruitment of PolY to form the SHE complex

Previously, we have shown assembly of the *Sso*PolB1 DNA polymerase holoenzyme (PolB1 HE) using presteady-state FRET (44). Assembly included a complex multiple step pathway to form the PolB1 HE complex. Although PolB1 has specificity for PCNA2 and PolY has specificity for PCNA1, we can also monitor binding to the heterotrimer PCNA123 and assembly of the complexes from either labelled position (Supplemental Figure S1A&B). Larger FRET is observed when there is a preformed PCNA123 heterotrimer with the label at either PCNA1 or PCNA2 subunit. From the clamp-loaded state (DNA/PCNA123/RFC), we have now monitored the recruitment of PolY to form the PolY TLS holoenzyme complex using specifically fluorescently labelled proteins (Supplemental Figure S1C). The averaged stopped-flow FRET trace fit best to a double exponential consistent with two conformational change steps (k_1^{obs} and k_2^{obs}) after association. PolY HE assembly can be monitored from either donor labeling of PCNA1, or PCNA2 with similar rate constants although labeling at PCNA2 ensures interaction FRET measurements with the PCNA123 trimer instead of direct interactions between PolY and PCNA1. Doubling or halving the PolY concentration did not significantly affect the observed rates (data not shown) indicating that we are monitoring second order conformational steps after binding.

When the PolB1 HE complex is preformed, addition of PolY to form the SHE complex can be monitored by FRET from multiple vantage points (Figure 3A). Specific labeling of DNA, PCNA1, PCNA2, or PolB1 with A^{488} within the PolB1 HE can be used as donor positions to follow an incoming PolY labeled with A^{594}. Interestingly, although the fluorescence amplitude changes as a function of labeling efficiency and relative spatial position within the SHE com-
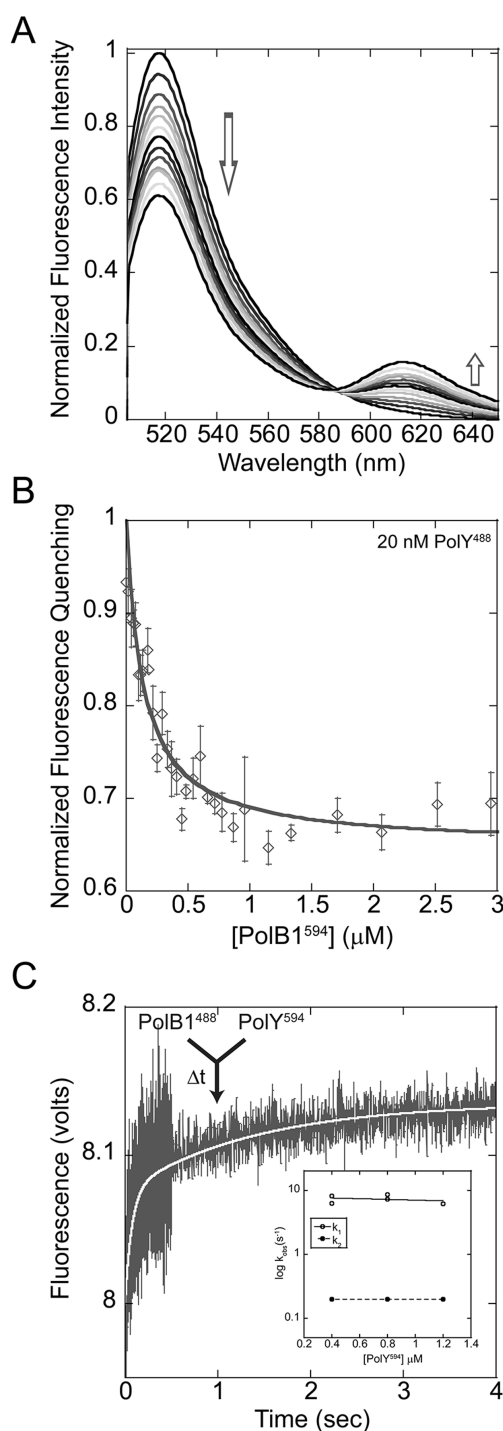
Figure 2. Direct Interaction of PolB1 and PolY Monitored by FRET. (**A**) Steady-state FRET quenching 20 nM PolY labeled with Alexa 488 (PolY^{488}) with PolB1 labeled with Alexa 594 (PolB1^{594}) at room temperature (22°C). Reported spectra were corrected for dilution and for the intrinsic fluorescence of buffer components and unlabeled PolY. Spectra were normalized to 1.0 by using the donor only as a reference. (**B**) The fluorescence maximum (@ 517 nm) was plotted as a function of [PolB1^{594}] and fit to Equation (1) to give $K_d = 0.14 \pm 0.02$ μM. Error bars represent the standard error from five independent titrations. (**C**) Presteady-state FRET of PolB1^{488} interacting with PolY^{594} (0.4 μM final) shows a biphasic curve. The observed rates (k_1 and k_2) from ten experiments consisting of at least seven averaged traces each were plotted as a function of [PolY^{594}] indicating second order rate constants (inset).
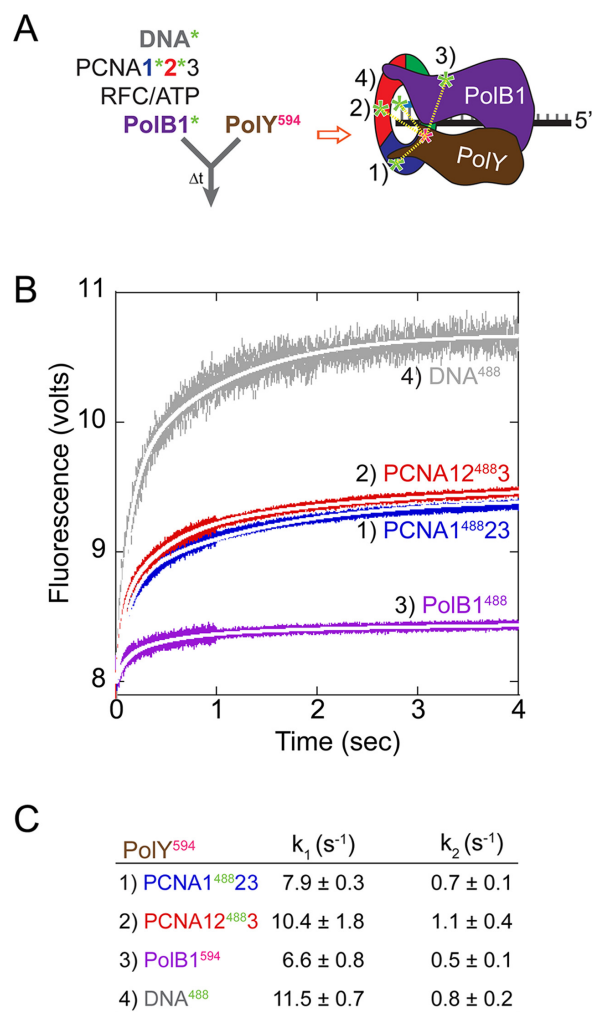

PolY^{594}	k_1 (s^{-1})	k_2 (s^{-1})
1) PCNA1^{488}23	7.9 ± 0.3	0.7 ± 0.1
2) PCNA12^{488}3	10.4 ± 1.8	1.1 ± 0.4
3) PolY^{594}	6.6 ± 0.8	0.5 ± 0.1
4) DNA^{488}	11.5 ± 0.7	0.8 ± 0.2

Figure 3. Presteady-state FRET Assembly of the SHE. (**A**) Presteady-state FRET traces monitoring interactions of PolY^{594} (0.4 μM final) to specific components of a preformed PolB1 HE complex. In each experiment, only one PolB1 HE component was fluorescent labeled with Alexa^{488} (*): DNA* (gray), PCNA2* (red), PCNA1* (blue) or PolB1* (purple) in separate experiments. (**B**) Fluorescence traces were adjusted to 8.0 and plotted together for more direct comparison of the (**C**) rates fit from a double exponential increase (Equation 2). Error values indicate the standard error from three independent experiments consisting of at least seven averaged traces each.

plex, the observed rates (k_1^{obs} and k_2^{obs}) are similar for binding of PolY (Figure 3B and C). This suggests that PolY binds the PolB1 HE complex independent of any one protein and that no single protein is displaced upon binding PolY. The DNA concentration in this experiment is limiting (0.2 μM final) as higher concentrations of DNA show vastly greater rates when DNA is labelled with A^{488}, more consistent with direct binding of PolY to free DNA. Changing the concentration of PolY while keeping the concentration of the PolB1 HE components the same does not alter the observed rates indicating that we are monitoring a first-order conformational change process (Supplemental Figure S2). Building on the kinetic assembly pathway from PolB1/PCNA123/DNA^G published previously (44), formation of the SHE complex proceeds through an equi-
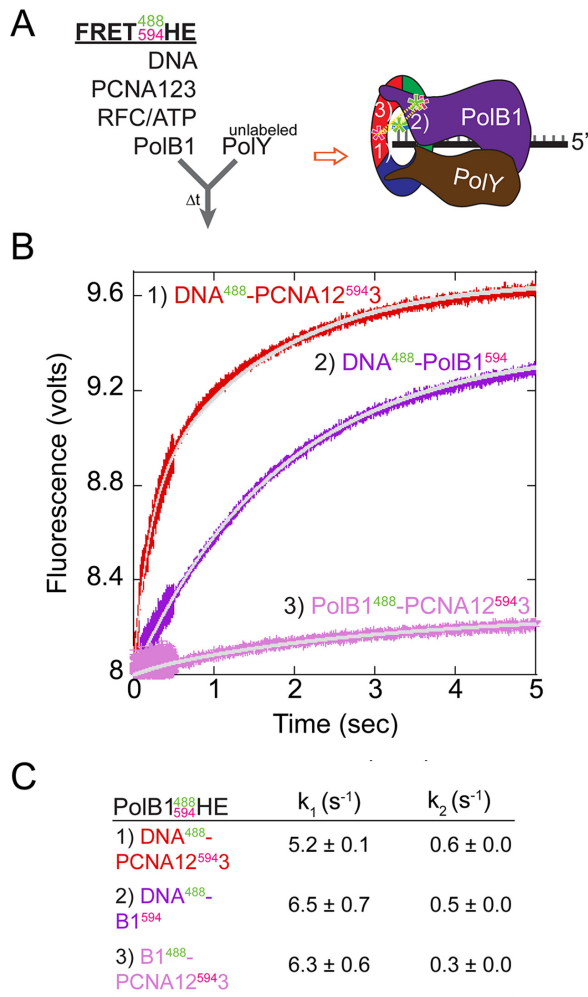
Figure 4. Addition of PolY Stabilizes the SHE Complex. (**A**) Preformed PolB1 HE with two of the components labeled was mixed with unlabeled PolY in a stopped-flow instrument and the FRET signal was monitored. (**B**) Presteady-state FRET traces of a preformed FRET PolB1 HE complex showing the fluorescence enhancement and stabilization upon addition of unlabeled PolY (0.4 μM final). Fluorescence traces were normalized to 8.0 for more direct comparison. Schematic representation of the FRET experiments is shown inset. (**C**) Double exponential rates (Equation 2) of the interactions fit for each FRET increase. Error values indicate the standard error from three independent experiments consisting of at least seven averaged traces each.

librium binding step (H) followed by two additional fluorescently observed conformational states (I-J).

In order to confirm that the PolB1 HE stays intact when PolY binds to form the SHE, we instead assembled a PolB1 HE labelled with both a donor and acceptor dye as a FRET complex from three different perspective and then mixed with unlabeled PolY (Figure 4A). In this experiment, should PolY displace the binding of any single PolB1 HE component, the FRET signal would decrease. However, for the three different experiments with donor and acceptor labels on different proteins or DNA, double exponential increases in fluorescence were observed (Figure 4B and C) that mirror the rates from direct FRET monitoring of SHE formation (Figure 3B). Therefore, PolY not only binds to form

the SHE complex, it also stabilizes and/or rearranges the overall conformation.

Polymerase exchange is directed by PIP interactions

Previously, we described how the *Sso* replicative holoenzyme achieves high rates of replication through a process of rapid polymerase re-recruitment, rather than processive single enzyme synthesis (44). This mechanism may also allow for the rapid exchange of the PolB1 replication polymerase with a TLS polymerase, PolY, opportunistically or specifically when needed. However, whether this is directed by contacts within a SHE complex or polymerase exchange occurs preferentially from solution is not known. Therefore, we titrated PolY constructs aimed to test interactions with PCNA into a PolB1 HE primer extension reaction (Figure 5). PolY has a slower global polymerization rate because of its low processivity (42); therefore, if it exchanges with PolB1, the product length will be shorter than as seen with WT (lanes 2–5). The reduction in product length occurs at stoichiometric or higher concentrations compared with PolB1. Mutation of the PIP site in PolY (PIP⁻) eliminates an interaction with PCNA1 specifically and shuts down DNA synthesis even more than WT (lanes 6–9) suggesting that either direct exchange from solution is favored or the PIP site interaction coordinates exchange within a SHE complex. Mutation of the active site of PolY (cat⁻) reduces product length further (lanes 10–13), consistent with both direct PolY exchange and with PCNA directed exchange within the SHE. Interestingly when the cat⁻/PIP⁻ PolY mutant was titrated, there was a partial rescue in product length (lanes 14–17) compared to cat⁻ alone (lanes 10–13) (Figure 5B and C), suggesting that PolY-PCNA1 contacts are important but not solely required for effective polymerase exchange. DNA synthesis was not inhibited until higher concentrations of the cat⁻/PIP⁻ polymerase were titrated compared to the cat⁻ PolY (Supplemental Figure S3). However, full length DNA products were not restored to WT lengths for cat⁻/PIP⁻ and were even greater than cat⁻ products, indicating that other interaction sites for PolY may exist within the SHE to mediate exchange. The combined data indicates that PolY is able to replace PolB1 from solution and that exchange is facilitated when PolY interacts with PCNA1, but importantly, there is also evidence for direct contacts between PolB1 and PolY within a SHE complex during active replication.

Novel PolB1-PolY (YB) interaction site identified within the supraholoenzyme

In order to probe a potential PolB1–PolY interaction on DNA synthesis ability and exchange, we identified residues (Y122, L126, I163) within a hydrophobic patch on the surface of PolY (Figure 6A and B). This patch was identified first through molecular modelling of a SHE complex that fixed the PIP site of PolB1 to PCNA2 and the PIP site of PolY to PCNA1 bound to a primer template DNA. We then utilized PolB1 truncation data that mapped PolY binding to the central region on PolB1 (residues 482–617) (21) to limit the potential interaction site of PolY contained with the SHE. Coincidently, these residues in Archaeal PolY are homologous to residues in the TLS polymerase, Pol IV, from
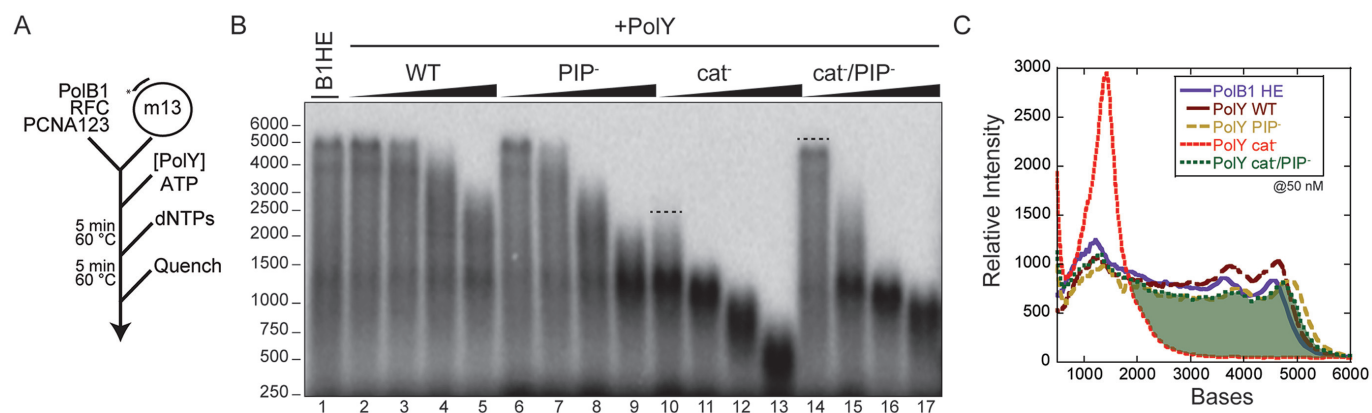
Figure 5. PolY PIP contacts are important for SHE action and exchange. (**A**) Experimental scheme showing PolY variants titrated to a 200 nM PolB1 HE before initiation with dNTPs to follow DNA synthesis length after five minutes at 60°C. (**B**) PolY WT, PIP⁻, cat⁻ or cat⁻/PIP⁻ were added at increasing concentration (50, 100, 200, 400 nM). The dashed lines (lanes 10 and 14) indicate C) the 50 nM [PolY] that are directly compared (cat⁻ versus cat⁻/PIP⁻) by difference shading (green) in quantification of the product lengths.
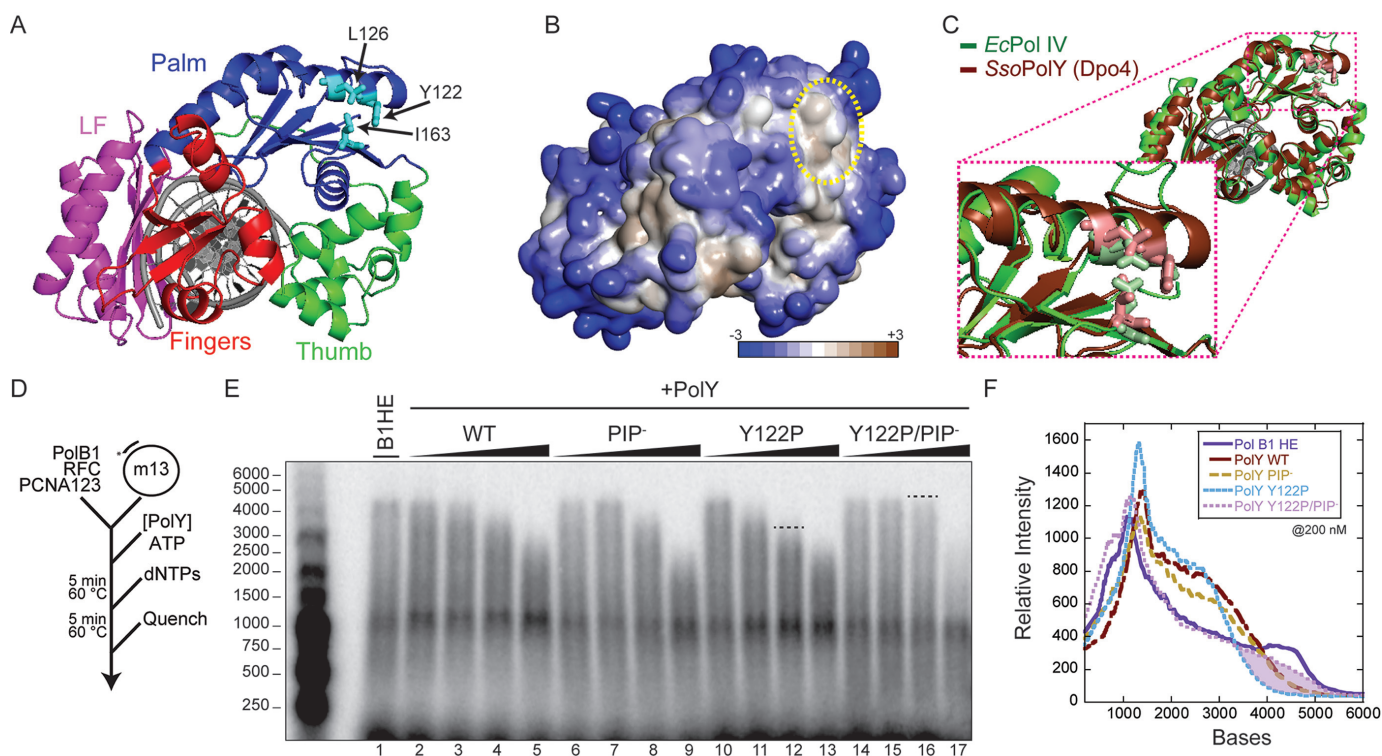

Figure 6. PolY YB contacts are also important for SHE action and exchange. (**A**) Crystal structure of *Sso*PolY(Dpo4)/DNA (PDBID: 1JXL) identifying residues (Y122, L126 and I163) within a (**B**) hydrophobic patch on the back of the palm domain. (**C**) Structural overlay of *Ec*Pol IV (PDBID: 4IR1) (green) with *Sso*PolY (brown) highlighting homologous Pol IV residues (T120, Q124 and Q161). (**D**) Experimental scheme showing PolY variants titrated to a 200 nM PolB1 holoenzyme before initiation with dNTPs to follow DNA synthesis length after 5 min at 60°C. (**E**) PolY WT, PIP⁻, Y122P, Y122P/PIP⁻ were added at increasing concentration (50, 100, 200, 400 nM). The dashed lines (lanes 12 and 16) indicate (**F**) the 200 nM [PolY] that are directly compared (Y122P vs. Y122P/PIP⁻) by difference shading (lilac) in quantification of the product lengths.

E. coli identified from a genetic mutant screen sensitive to DNA damage (19) (Figure 6C).

Again, we designed primer extension assays to test the ability of these PolY mutants (Y122A, Y122P, L126N, I163N) to direct exchange within the SHE complex and slow synthesis to affect product length. The absence of an interaction of PolY with PolB1 from a specific mutation would abrogate this polymerase exchange ability and result in longer products than with wild-type PolY. Mutation of PolY (Y122P) decreases the quenching and binding affinity for PolB1 measured in steady-state FRET assay (Supplemental Figure S4). In fact when each of the PolY mutants was titrated into a PolB1 HE primer extension assay, only in combination with the PIP⁻ mutation did the PolY–
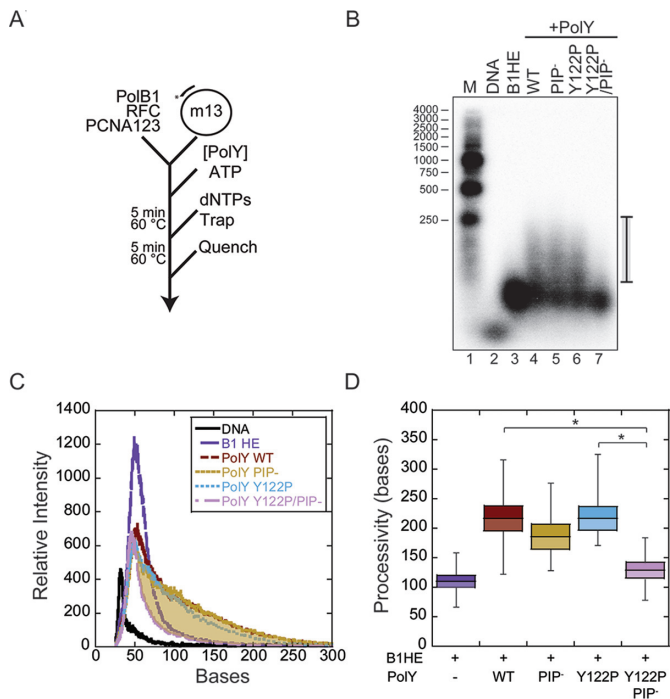
Figure 7. Addition of PolY Increases the Processivity of the PolB1 HE. (**A**) Experimental scheme showing (**B**) 200 nM PolY variants [WT (brown), PIP⁻ (maize), Y122P (azure), Y122P/PIP⁻ (lilac)] added to a 200 nM PolB1 HE before initiation with dNTPs and 3 mg/ml ssDNA trap to follow processivity of DNA synthesis. (**C**) Quantification of the DNA product lengths and difference shading (maize) of Y122P/PIP⁻ compared to PIP⁻. (**D**) Plot of the mean, standard error and range of processivity values for SHE combinations from eight independent experiments. Significance and *P*-values are indicated (* 0.5).

YB/PIP⁻ mutants restore more full length product at the higher concentrations, indicating the exchange had been affected (Supplemental Figure S5). Directly comparing stoichiometric concentrations of PolB1 and PolY in this assay for Y122P and Y122P/PIP⁻ mutants show only a restoration of product length when both contact sites in PolY are mutated (lanes 14–17) (Figure 6D–F). Quantification of the product length as a function of concentration of each PolY construct shows modulation in the product length, especially for Y122P/PIP⁻ (Supplemental Figure S6). Therefore, PolY requires at a minimum interactions with both PCNA1 (PIP) and PolB1 (YB) to direct exchange from solution and within the SHE complex.

Based on the stabilization of the SHE complex noted above with the stopped-flow FRET (Figure 4) and the YB contacts identified to be important for complex formation, we next tested the ability of the SHE complex to increase processivity of DNA synthesis (Figure 7). Previously, we had shown that the PolB1 HE alone has low processivity and instead acts distributively during synthesis, repetitively recruiting PolB1 to replicate long stretches of DNA (44). Addition of WT PolY to the PolB1 HE (forming the SHE) increases the processivity of DNA synthesis by a few hundred bases (lanes 3 versus 4) (Figure 7B). In these processivity assays, a high concentration of ssDNA is added with the dNTPs to initiate synthesis while at the same time trapping any polymerases that dissociate from the DNA tem-
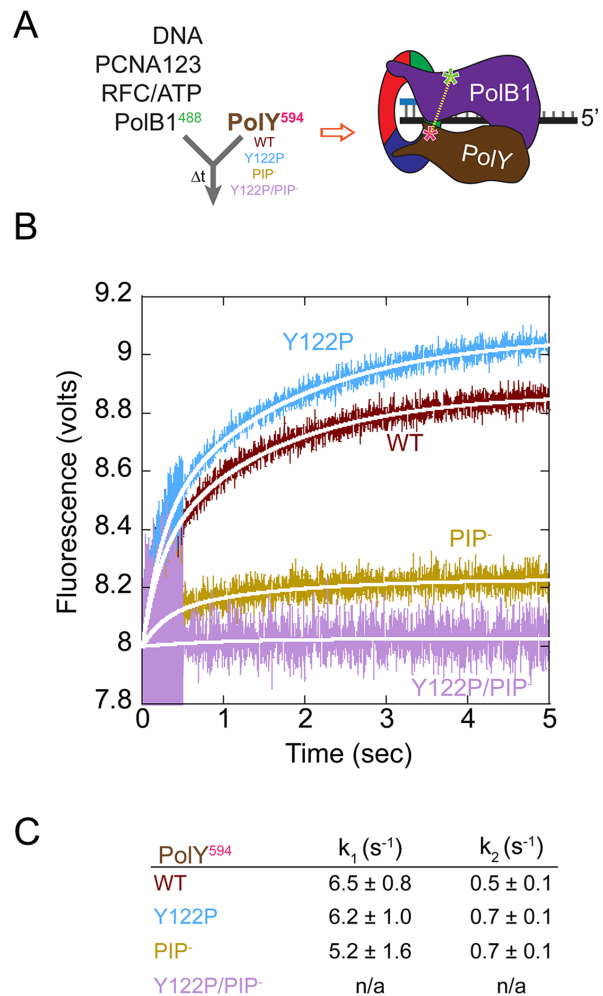

Figure 8. SHE Formation is Dependent on Both PIP and YB Sites. Presteady-state FRET traces showing the interactions of PolY⁵⁹⁴ [WT (brown), PIP⁻ (maize), Y122P (azure), Y122P/PIP⁻ (lilac)] to Pol B1⁴⁸⁸ HE. (**A**) Fluorescence traces were normalized to 8.0 for more direct comparison and fit to a double exponential (Equation 2) and reported in (**B**). Error values indicate the standard error from three independent experiments consisting of at least seven averaged traces each.

plate during the course of the reaction to measure length of DNA synthesis from a single processive event. Both PIP⁻ and Y122P PolY constructs also increase the processivity significantly over PolB1 HE alone (Figure 7B, lanes 5–6 and C). However, when both PIP⁻ and Y122P mutations are combined, the processivity is reduced to PolB1 HE level (lanes 3 versus 7) implicating both sites for the stabilization of the SHE complex on DNA.

Presteady-state stopped-flow FRET experiments were used again to follow the impact of the Y122P on interaction within the PolB1 HE. PolY Y122P interacts similarly to WT with PCNA123 labelled at PCNA1 or PCNA2 in isolation (Supplemental Figure S7). When PolB1⁴⁸⁸ was preloaded on DNA in a HE complex and rapidly mixed with PolY⁵⁹⁴ (WT or Y122P), there were similar double exponential increases observed (Figure 8). The amplitude is consistently larger for Y122P over WT, which may indicate a slightly different final conformation for this mutant within the SHE

complex. Mutation of PIP⁻ in PolY reduces the FRET signal considerably but without significantly affecting the rate, suggesting a reduction in the formation of the SHE complex. The combination of Y122P and PIP⁻ mutations in PolY virtually abrogate the entire FRET signal, clearly implicating both the PIP and YB sites in formation of the SHE complex.

DISCUSSION

In this study, we have identified interactions between the B-family replication polymerase and the Y-family TLS polymerase in *Sso* that contribute to formation of a supra-holoenzyme (SHE) complex. For this, we utilized a combination of biochemical techniques aimed at first identifying direct interactions between polymerases first by analytical gel filtration and FRET and second examining the mechanism of polymerase exchange that occurs during DNA synthesis. Known PIP binding sites to PCNA1 as well as a newly identified YB interaction site between polymerases are together required for maintaining the SHE complex. The YB site is a conserved hydrophophic patch on the back of the palm domain of PolY. Binding of PolY to the PolB1 HE occurs through concerted interactions with the PIP interaction site on PCNA1 and a YB interaction site with PolB1. The presence of PolY within the SHE stabilizes the entire complex, effectively increasing processivity of DNA synthesis. Direct polymerase exchange with the DNA template can occur within the confines of the SHE complex during DNA synthesis repetitively switching high and low fidelity polymerases. At higher concentrations of PolY, polymerase exchange from solution predominates, displacing the PolB1 HE or SHE. Identification of the SHE complex expands our understanding of concerted DNA polymerase exchange within the complex as well as provides a plausible mechanism for recruitment of PolY from solution for coordination of high fidelity and translesion DNA synthesis.

PCNA is known to interact with many protein partners through the PIP binding site, however, how the trimeric protein coordinates binding and regulates activity is still not known. The availability of three binding sites on the trimer could allow up to three different protein partners to be contained and their activities coordinated towards the DNA substrate in a 'tool-belt' configuration. Increasing local concentrations of proteins or providing contacts for recruitment by simultaneous binding to PCNA can effectively increase the rate of processing. For example, Okazaki fragment maturation requires the sequential action of DNA polymerase, flap endonuclease, and DNA ligase. In archaea, it has been shown that an Okazakisome consisting of the co-occupancy of these three proteins to the heterotrimeric *Sso*PCNA123 can exist to promote joining of Okazaki fragments (39,47). However, although a similar Okazaki fragment maturation complex can exist in eukaryotes, engineered single binding site PCNA molecules are fully capable of directing lagging-strand processing through a sequential switching process (48,49) calling into question the absolute utility of the 'tool-belt'.

Perhaps some of the most well characterized 'tool-belt' activity and coordination comes from work with the beta-clamp and various DNA polymerases in bacteria. Both the

high-fidelity Pol III and lower-fidelity TLS Pol IV can be contained on the beta clamp (41) and a secondary binding site can regulate Pol IV engagement and Pol III dissociation at the site of a lesion (50–53). In the absence of Pol IV or on undamaged DNA, Pol III preferentially engages the DNA template for active and processive DNA synthesis. Further work identified a functional interaction between residues in Pol III and Pol IV from a genetic screen (19) that are homologous to the YB site identified here (Figure 6C). In addition to Pol IV, the cryptic activity of the TLS Pol II has also been shown to form a 'tool-belt' complex with Pol III and the beta clamp that can rapidly exchange binding to the DNA template, although the disruptive activity is less than for Pol IV (20). The third TLS polymerase in bacteria, Pol V, can also be bound to the beta clamp through an opposite cleft from Pol III, however, genetic experiments show that a single cleft is capable of supporting coordinated TLS synthesis implicating other binding sites within this complex (54). Pol V–Pol III directed exchange and TLS coordination has yet to be shown experimentally *in vitro*.

It is interesting that different laboratories have independently identified common polymerase interaction sites (YB) in two highly divergent domains of life: bacteria and archaea. The amino acid residues in this area are not highly homologous across domains or even within related species. However from the limited X-ray structures available, there is a strong hydrophobic surface on the back of the palm domain of all these polymerases. As well as providing for an interaction with PolB1 (YB) within a SHE complex, this hydrophobic patch may also be important for recruiting PolY to additional DNA damaged sites through interactions with other proteins such as single-strand binding protein or other DNA repair factors.

PolY's primary interaction site is with the clamp protein, i.e. PCNA1 in *Sso*. The co-occupancy of two polymerases on the clamp (especially Pol III and Pol IV) has been shown to be dynamic, with both polymerases switching access to the DNA template and influencing the dissociation of the other (50,51). The consequences of co-occupancy of polymerases must include having at least two conformational states: DNA engaged and unengaged. High fidelity proof-reading polymerases must also have at least two additional engaged conformational states for polymerase and exonuclease activities. The dynamics and coordination of all of these conformational states are not entirely clear, however, archaeal *Pyrococcus furiosus* PolB has been visualized by EM in different conformation states identifying additional interactions with PCNA that position it in a 'standby' state that is unengaged from DNA (55,56). Moreover, hinges in *Sso*PolY (Dpo4) have also been shown to influence the conformation of PolY bound to PCNA/DNA complex indicating at least three conformational states that regulate the activity and accessibility to DNA (43). These alternative conformational states could allow for binding of both *Sso* PolB1 to PolY in the SHE complex and allow for 'tool-belt' – like polymerase switching to occur that seamlessly replicates undamaged DNA and bypasses lesions.

In eukaryotes, stalled DNA polymerases at DNA lesions will cause an increase in the amount of ssDNA created, and the buildup and persistence of RPA-coated DNA which is a signal for the Rad6/Rad18 dependent monoubiquitination

(mUb) of PCNA (57–59). Whether this later stage temporal process is what actually directs TLS activity or just upregulates the global DNA damage response (DDR) in severe cases is still being determined. For example, the human Y-family pol η is known to colocalize with DNA replication foci even in undamaged conditions (8), and the ubiquitination of PCNA is not required for the localization of pol η in foci (60). Although in humans there is no current evidence for a SHE-like complex, translesion synthesis can occur 'on the fly' and without mUB through a passive exchange mechanism with pol δ (59,61,62). This passive exchange mechanism relies on the inherent dissociation property of pol δ at a lesion site allowing for pol η to bind in its place. Whether pol η or any other Y-family pol influences this dissociation or exchange is still being studied. Therefore, the emerging view is that 'on the fly' TLS activity can be coordinated within the progressing replisome with associated Y-family pols, while more extreme stalling or replication re-start may require mUB of PCNA for more stable recruitment of Y-family pols. This is similar in principle to the archaeal SHE complex identified here.

In conclusion, our study identifies and characterizes a PCNA 'tool-belt' configuration of high fidelity PolB1 and TLS PolY polymerases simultaneously contained within a SHE complex in archaea. This novel YB interaction site between polymerases and in combination with the PIP sites are important for the processivity of the entire complex and exchange processes that occur both within the SHE complex as well as from solution. The implication of the SHE complex provides a mechanism for coordinating and localizing replication and TLS activities at the replication fork. It still remains to be seen how this polymerase coordination actually contributes to efficient TLS activity both *in vitro* and *in vivo* and whether similar mechanisms exist in eukaryotic systems or whether archaea and bacteria share sole homology for this process.

SUPPLEMENTARY DATA

Supplementary Data are available at NAR Online.

ACKNOWLEDGEMENTS

We are grateful to P.F. Guengerich for providing antibodies to *Sso*PolY and *Sso*PolB1. We acknowledge the Baylor Molecular Bioscience Center (MBC) for providing instrumentation and resources aiding this project.
Author contributions: M.T.C. and R.J.B. performed mutagenesis, protein purification, and kinetic replication and processivity assays. A.M.C. performed mutagenesis, protein purification, analytical gel filtration, fluorescent labeling, steady-state, and stopped-flow experiments. J.K.B. performed protein mutagenesis and purification. M.A.T. designed the experimental approach and wrote the paper. All authors analyzed data, prepared figures and edited the manuscript.

FUNDING

REFERENCES

1. Ohmori,H., Friedberg,E.C., Fuchs,R.P., Goodman,M.F., Hanaoka,F., Hinkle,D., Kunkel,T.A., Lawrence,C.W., Livneh,Z., Nohmi,T. *et al.* (2001) The Y-family of DNA polymerases. *Mol. Cell*, **8**, 7–8.
2. Prakash,S., Johnson,R.E. and Prakash,L. (2005) Eukaryotic translesion synthesis DNA polymerases: Specificity of structure and function. *Annu. Rev. Biochem.*, **74**, 317–353.
3. Sale,J.E., Lehmann,A.R. and Woodgate,R. (2012) Y-family DNA polymerases and their role in tolerance of cellular DNA damage. *Nat. Rev. Mol. Cell Biol.*, **13**, 141–152.
4. Liu,B., Xue,Q., Tang,Y., Cao,J., Guengerich,F.P. and Zhang,H. (2016) Mechanisms of mutagenesis: DNA replication in the presence of DNA damage. *Mutat. Res. Rev. Mutat. Res.*, **768**, 53–67.
5. Boehm,E.M., Gildenberg,M.S. and Washington,M.T. (2016) The many roles of PCNA in eukaryotic DNA replication. *Enzymes*, **39**, 231–254.
6. Maga,G. and Hubscher,U. (2003) Proliferating cell nuclear antigen (PCNA): a dancer with many partners. *J. Cell Sci.*, **116**, 3051–3060.
7. Moldovan,G.L., Pfander,B. and Jentsch,S. (2007) PCNA, the maestro of the replication fork. *Cell*, **129**, 665–679.
8. Bienko,M., Green,C.M., Crosetto,N., Rudolf,F., Zapart,G., Coull,B., Kannouche,P., Wider,G., Peter,M., Lehmann,A.R. *et al.* (2005) Ubiquitin-binding domains in Y-family polymerases regulate translesion synthesis. *Science*, **310**, 1821–1824.
9. Hendel,A., Krijger,P.H., Diamant,N., Goren,Z., Langerak,P., Kim,J., Reissner,T., Lee,K.Y., Geacintov,N.E., Carell,T. *et al.* (2011) PCNA ubiquitination is important, but not essential for translesion DNA synthesis in mammalian cells. *PLoS Genet.*, **7**, e1002262.
10. Pryor,J.M., Dieckman,L.M., Boehm,E.M. and Washington,M.T. (2014) In: Murakami,KS and Trakselis,MA (eds). *Nucleic Acids Mol Bi*. Springer-Verlag, Berlin, Vol. 30, pp. 85–108.
11. Masuda,Y., Kanao,R., Kaji,K., Ohmori,H., Hanaoka,F. and Masutani,C. (2015) Different types of interaction between PCNA and PIP boxes contribute to distinct cellular functions of Y-family DNA polymerases. *Nucleic Acids Res.*, **43**, 7898–7910.
12. Plosky,B.S., Vidal,A.E., Fernandez de Henestrosa,A.R., McLenigan,M.P., McDonald,J.P., Mead,S. and Woodgate,R. (2006) Controlling the subcellular localization of DNA polymerases iota and eta via interactions with ubiquitin. *EMBO J.*, **25**, 2847–2855.
13. Despras,E., Delrieu,N., Garandeau,C., Ahmed-Seghir,S. and Kannouche,P.L. (2012) Regulation of the specialized DNA polymerase eta: revisiting the biological relevance of its PCNA- and ubiquitin-binding motifs. *Environ. Mol. Mutagen.*, **53**, 752–765.
14. Freudenthal,B.D., Gakhar,L., Ramaswamy,S. and Washington,M.T. (2010) Structure of monoubiquitinated PCNA and implications for translesion synthesis and DNA polymerase exchange. *Nat. Struct. Mol. Biol.*, **17**, 479–484.
15. Garg,P. and Burgers,P.M. (2005) Ubiquitinated proliferating cell nuclear antigen activates translesion DNA polymerases eta and REV1. *Proc. Natl. Acad. Sci. U.S.A.*, **102**, 18361–18366.
16. Matsumiya,S., Ishino,S., Ishino,Y. and Morikawa,K. (2002) Physical interaction between proliferating cell nuclear antigen and replication factor C from *Pyrococcus furiosus*. *Genes Cells*, **7**, 911–922.
17. Williams,G.J., Johnson,K., Rudolf,J., McMahon,S.A., Carter,L., Oke,M., Liu,H., Taylor,G.L., White,M.F. and Naismith,J.H. (2006) Structure of the heterotrimeric PCNA from *Sulfolobus solfataricus*. *Acta Crystallograph. Sect. F. Struct. Biol. Cryst. Commun.*, **62**, 944–948.
18. Jeruzalmi,D., Yurieva,O., Zhao,Y., Young,M., Stewart,J., Hingorani,M., O'Donnell,M. and Kuriyan,J. (2001) Mechanism of processivity clamp opening by the delta subunit wrench of the clamp loader complex of *E.coli* DNA polymerase III. *Cell*, **106**, 417–428.
19. Scotland,M.K., Heltzel,J.M., Kath,J.E., Choi,J.S., Berdis,A.J., Loparo,J.J. and Sutton,M.D. (2015) A genetic selection for dinB mutants reveals an interaction between DNA polymerase IV and the replicative polymerase that is required for translesion synthesis. *PLoS Genet.*, **11**, e1005507.

20. Kath,J.E., Chang,S., Scotland,M.K., Wilbertz,J.H., Jergic,S., Dixon,N.E., Sutton,M.D. and Loparo,J.J. (2016) Exchange between *Escherichia coli* polymerases II and III on a processivity clamp. *Nucleic Acids Res.*, **44**, 1681–1690.

21. De Felice,M., Medagli,B., Esposito,L., De Falco,M., Pucci,B., Rossi,M., Gruz,P., Nohmi,T. and Pisani,F.M. (2007) Biochemical evidence of a physical interaction between *Sulfolobus solfataricus* B-family and Y-family DNA polymerases. *Extremophiles*, **11**, 277–282.

22. Lin,H.K., Chase,S.F., Laue,T.M., Jen-Jacobson,L. and Trakselis,M.A. (2012) Differential temperature-dependent multimeric assemblies of replication and repair polymerases on DNA increase processivity. *Biochemistry*, **51**, 7367–7382.

23. Mikheikin,A.L., Lin,H.K., Mehta,P., Jen-Jacobson,L. and Trakselis,M.A. (2009) A trimeric DNA polymerase complex increases the native replication processivity. *Nucleic Acids Res.*, **37**, 7194–7205.

24. Lopez de Saro,F.J., Georgescu,R.E., Goodman,M.F. and O'Donnell,M. (2003) Competitive processivity-clamp usage by DNA polymerases during DNA replication and repair. *EMBO J.*, **22**, 6408–6418.

25. Makarova,K.S. and Koonin,E.V. (2013) Archaeology of eukaryotic DNA replication. *Cold Spring Harbor Perspect. Biol.*, **5**, a012963.

26. Hug,L.A., Baker,B.J., Anantharaman,K., Brown,C.T., Probst,A.J., Castelle,C.J., Butterfield,C.N., Hernsdorf,A.W., Amano,Y., Ise,K. *et al.* (2016) A new view of the tree of life. *Nat. Microbiol.*, **1**, 16048.

27. Ling,H., Boudsocq,F., Woodgate,R. and Yang,W. (2001) Crystal structure of a Y-family DNA polymerase in action: a mechanism for error-prone and lesion-bypass replication. *Cell*, **107**, 91–102.

28. Boudsocq,F., Iwai,S., Hanaoka,F. and Woodgate,R. (2001) *Sulfolobus solfataricus* P2 DNA polymerase IV (Dpo4): an archaeal DinB-like DNA polymerase with lesion-bypass properties akin to eukaryotic poleta. *Nucleic Acids Res.*, **29**, 4607–4616.

29. Kokoska,R.J., Bebenek,K., Boudsocq,F., Woodgate,R. and Kunkel,T.A. (2002) Low fidelity DNA synthesis by a Y-family DNA polymerase due to misalignment in the active site. *J. Biol. Chem.*, **277**, 19633–19638.

30. Ling,H., Boudsocq,F., Woodgate,R. and Yang,W. (2004) Snapshots of replication through an abasic lesion; structural basis for base substitutions and frameshifts. *Mol. Cell*, **13**, 751–762.

31. Fiala,K.A. and Suo,Z. (2004) Mechanism of DNA polymerization catalyzed by *Sulfolobus solfataricus* P2 DNA polymerase IV. *Biochemistry*, **43**, 2116–2125.

32. Eoff,R.L., Sanchez-Ponce,R. and Guengerich,F.P. (2009) Conformational changes during nucleotide selection by *Sulfolobus solfataricus* DNA polymerase Dpo4. *J. Biol. Chem.*, **284**, 21090–21099.

33. Maxwell,B.A. and Suo,Z. (2012) Kinetic basis for the differing response to an oxidative lesion by a replicative and a lesion bypass DNA polymerase from *Sulfolobus solfataricus*. *Biochemistry*, **51**, 3485–3496.

34. Boudsocq,F., Kokoska,R.J., Plosky,B.S., Vaisman,A., Ling,H., Kunkel,T.A., Yang,W. and Woodgate,R. (2004) Investigating the role of the little finger domain of Y-family DNA polymerases in low fidelity synthesis and translesion replication. *J. Biol. Chem.*, **279**, 32932–32940.

35. Sholder,G., Creech,A. and Loechler,E.L. (2015) How Y-Family DNA polymerase IV is more accurate than Dpo4 at dCTP insertion opposite an N2-dG adduct of benzo[a]pyrene. *DNA Repair (Amst.)*, **35**, 144–153.

36. Walsh,J.M., Ippoliti,P.J., Ronayne,E.A., Rozners,E. and Beuning,P.J. (2013) Discrimination against major groove adducts by Y-family polymerases of the DinB subfamily. *DNA Repair (Amst.)*, **12**, 713–722.

37. Wilson,R.C., Jackson,M.A. and Pata,J.D. (2013) Y-family polymerase conformation is a major determinant of fidelity and translesion specificity. *Structure*, **21**, 20–31.

38. Dionne,I., Nookala,R.K., Jackson,S.P., Doherty,A.J. and Bell,S.D. (2003) A heterotrimeric PCNA in the hyperthermophilic archaeon *Sulfolobus solfataricus*. *Mol. Cell*, **11**, 275–282.

39. Beattie,T.R. and Bell,S.D. (2012) Coordination of multiple enzyme activities by a single PCNA in archaeal Okazaki fragment maturation. *EMBO J.*, **31**, 1556–1567.

40. Dore,A.S., Kilkenny,M.L., Jones,S.A., Oliver,A.W., Roe,S.M., Bell,S.D. and Pearl,L.H. (2006) Structure of an archaeal PCNA1-PCNA2-FEN1 complex: Elucidating PCNA subunit and client enzyme specificity. *Nucleic Acids Res.*, **34**, 4515–4526.

41. Indiani,C., McInerney,P., Georgescu,R., Goodman,M.F. and O'Donnell,M. (2005) A sliding-clamp toolbelt binds high- and low-fidelity DNA polymerases simultaneously. *Mol. Cell*, **19**, 805–815.

42. Choi,J.Y., Eoff,R.L., Pence,M.G., Wang,J., Martin,M.V., Kim,E.J., Folkmann,L.M. and Guengerich,F.P. (2011) Roles of the four DNA polymerases of the crenarchaeon *Sulfolobus solfataricus* and accessory proteins in DNA replication. *J. Biol. Chem.*, **286**, 31180–31193.

43. Xing,G., Kirouac,K., Shin,Y.J., Bell,S.D. and Ling,H. (2009) Structural insight into recruitment of translesion DNA polymerase Dpo4 to sliding clamp PCNA. *Mol. Microbiol.*, **71**, 678–691.

44. Bauer,R.J., Wolff,I.D., Zuo,X., Lin,H.K. and Trakselis,M.A. (2013) Assembly and distributive action of an archaeal DNA polymerase holoenzyme. *J. Mol. Biol.*, **425**, 4820–4836.

45. Studier,F.W. (2005) Protein production by auto-induction in high density shaking cultures. *Protein Expression Purif.*, **41**, 207–234.

46. Brenlla,A., Markiewicz,R.P., Rueda,D. and Romano,L.J. (2014) Nucleotide selection by the Y-family DNA polymerase Dpo4 involves template translocation and misalignment. *Nucleic Acids Res.*, **42**, 2555–2563.

47. Cannone,G., Xu,Y., Beattie,T.R., Bell,S.D. and Spagnolo,L. (2015) The architecture of an Okazaki fragment-processing holoenzyme from the archaeon Sulfolobus solfataricus. *Biochem. J.*, **465**, 239–245.

48. Dovrat,D., Stodola,J.L., Burgers,P.M. and Aharoni,A. (2014) Sequential switching of binding partners on PCNA during in vitro Okazaki fragment maturation. *Proc. Natl. Acad. Sci. U.S.A.*, **111**, 14118–14123.

49. Stodola,J.L. and Burgers,P.M. (2016) Resolving individual steps of Okazaki-fragment maturation at a millisecond timescale. *Nat. Struct. Mol. Biol.*, **23**, 402–408.

50. Kath,J.E., Jergic,S., Heltzel,J.M., Jacob,D.T., Dixon,N.E., Sutton,M.D., Walker,G.C. and Loparo,J.J. (2014) Polymerase exchange on single DNA molecules reveals processivity clamp control of translesion synthesis. *Proc. Natl. Acad. Sci. U.S.A.*, **111**, 7647–7652.

51. Furukohri,A., Goodman,M.F. and Maki,H. (2008) A dynamic polymerase exchange with *Escherichia coli* DNA polymerase IV replacing DNA polymerase III on the sliding clamp. *J. Biol. Chem.*, **283**, 11260–11269.

52. Heltzel,J.M., Maul,R.W., Scouten Ponticelli,S.K. and Sutton,M.D. (2009) A model for DNA polymerase switching involving a single cleft and the rim of the sliding clamp. *Proc. Natl. Acad. Sci. U.S.A.*, **106**, 12664–12669.

53. Bunting,K.A., Roe,S.M. and Pearl,L.H. (2003) Structural basis for recruitment of translesion DNA polymerase Pol IV/DinB to the beta-clamp. *EMBO J.*, **22**, 5883–5892.

54. Sutton,M.D., Duzen,J.M. and Scouten Ponticelli,S.K. (2010) A single hydrophobic cleft in the *Escherichia coli* processivity clamp is sufficient to support cell viability and DNA damage-induced mutagenesis *in vivo*. *BMC Mol. Biol.*, **11**, 102.

55. Mayanagi,K., Kiyonari,S., Nishida,H., Saito,M., Kohda,D., Ishino,Y., Shirai,T. and Morikawa,K. (2011) Architecture of the DNA polymerase B-proliferating cell nuclear antigen (PCNA)-DNA ternary complex. *Proc. Natl. Acad. Sci. U.S.A.*, **108**, 1845–1849.

56. Nishida,H., Mayanagi,K., Kiyonari,S., Sato,Y., Oyama,T., Ishino,Y. and Morikawa,K. (2009) Structural determinant for switching between the polymerase and exonuclease modes in the PCNA-replicative DNA polymerase complex. *Proc. Natl. Acad. Sci. U.S.A.*, **106**, 20693–20698.

57. Chang,D.J., Lupardus,P.J. and Cimprich,K.A. (2006) Monoubiquitination of proliferating cell nuclear antigen induced by stalled replication requires uncoupling of DNA polymerase and mini-chromosome maintenance helicase activities. *J. Biol. Chem.*, **281**, 32081–32088.

58. Davies,A.A., Huttner,D., Daigaku,Y., Chen,S. and Ulrich,H.D. (2008) Activation of ubiquitin-dependent DNA damage bypass is mediated by replication protein a. *Mol. Cell*, **29**, 625–636.

59. Hedglin,M. and Benkovic,S.J. (2015) Regulation of Rad6/Rad18 activity during DNA damage tolerance. *Annu. Rev. Biophys.*, **44**, 207–228.

60. Sabbioneda,S., Gourdin,A.M., Green,C.M., Zotter,A., Giglia-Mari,G., Houtsmuller,A., Vermeulen,W. and Lehmann,A.R.

(2008) Effect of proliferating cell nuclear antigen ubiquitination and chromatin structure on the dynamic properties of the Y-family DNA polymerases. *Mol. Biol. Cell*, **19**, 5193–5202.

61. Edmunds,C.E., Simpson,L.J. and Sale,J.E. (2008) PCNA ubiquitination and REV1 define temporally distinct mechanisms for controlling translesion synthesis in the avian cell line DT40. *Mol. Cell*, **30**, 519–529.

62. Hedglin,M., Pandey,B. and Benkovic,S.J. (2016) Characterization of human translesion DNA synthesis across a UV-induced DNA lesion. *Elife*, **5**, e19788.